

Single-Crystal Cobalt-59 NMR Study of Tris(2,4-pentanedionato-*O,O'*)cobalt(III)

Klaus Eichele,[†] Jerry C. C. Chan,[†] Roderick E. Wasylishen,^{*,†} and James F. Britten[‡]

Department of Chemistry, Dalhousie University, Halifax, Nova Scotia, Canada B3H 4J3, and Department of Chemistry, McMaster University, Hamilton, Ontario, Canada L8S 4M1

Received: January 30, 1997; In Final Form: May 15, 1997[⊗]

Cobalt-59 NMR spectra of a single crystal of tris(2,4-pentanedionato-*O,O'*) cobalt(III) were obtained as a function of crystal orientation in an applied magnetic field of 9.40 T. The analysis provides the magnitudes and orientations of the ⁵⁹Co nuclear quadrupole coupling and chemical shift tensors for each of the two magnetically distinct but crystallographically equivalent cobalt sites. The cobalt electric field gradient and chemical shift tensors are not coincident, but their unique components are close to the approximate *C*₃ axis of the complex. Small deviations from perfect octahedral symmetry at the cobalt nucleus result in a significant nuclear electric field gradient and highly anisotropic chemical shift. The cobalt nuclear quadrupolar coupling constant is 5.53 ± 0.10 MHz with an asymmetry of 0.219 ± 0.005, while the chemical shift tensor has a span of 1174 ± 25 ppm. The principal components relative to the isotropic chemical shift, $\delta_{\text{iso}} = 12498 \pm 5$ ppm, are $\delta_{11} = 698 \pm 22$ ppm, $\delta_{22} = -222 \pm 12$ ppm, and $\delta_{33} = -476 \pm 5$ ppm. The quadrupolar tensor was characterized by examining splittings between the satellite transitions, while the chemical shift tensor was characterized by analyzing the central transition and correcting for the second-order quadrupolar interaction. The results obtained in this study are compared with those of previous ⁵⁹Co NMR studies.

Introduction

The nuclear magnetic resonance (NMR) periodic table is dominated by quadrupolar nuclei (spin $I \geq 1$) and of these, almost all have noninteger spin.¹ NMR spectra of quadrupolar nuclei in the solid state are of particular interest because they give experimentalists a unique opportunity to simultaneously investigate the electric field gradient (EFG) and chemical shift (CS) tensors at a nuclear site. Sites at which the crystal structure places no symmetry constraints on the orientation of these tensors have attracted much recent attention.^{2–7} General procedures for the analysis of NMR spectra arising from powder samples are a challenge and require well-characterized systems to assess their applicability. Parallel to this activity, there have been tremendous advances in computational chemistry which now make it possible for theoreticians to calculate EFG and CS tensors at nuclei well beyond the first row of the periodic table.^{8,9} Reliable calculations of both EFG and CS tensors require an accurate description of electronic structure in the vicinity of the nucleus. Furthermore, the electric field gradient is a ground-state, first-order property while the chemical shift is a second-order property.¹⁰ In order to test state-of-the-art computations it is imperative to have well-established experimental benchmarks. The objective of the present study is to characterize the ⁵⁹Co nuclear quadrupolar coupling and chemical shift tensors for solid tris(2,4-pentanedionato-*O,O'*)cobalt(III), also known as tris(acetylacetonato)cobalt(III) or Co(acac)₃.

Cobalt-59 is a spin $7/2$ nucleus with a natural abundance of 100% and relatively large magnetic and nuclear quadrupole moments. Cobalt NMR is of historic interest because in their 1951 study of nuclear magnetic moments, Proctor and Yu¹¹ noted variations in ⁵⁹Co NMR resonance frequencies amounting to as much as 1.3%. A theoretical interpretation of cobalt chemical shifts, based on crystal-field theory, was first given

in 1957 by Griffith and Orgel¹² and by Freeman, Murray, and Richards.¹³ Cobalt(III) complexes have a chemical shift range in excess of 12 000 ppm.¹⁴ In such complexes, ⁵⁹Co nuclei surrounded by six oxygen donor ligands are among the least shielded. Our investigation of Co(acac)₃ was prompted by inconsistencies in the ⁵⁹Co NMR parameters previously reported for this compound (*vide infra*).

The first ⁵⁹Co NMR study of solid Co(acac)₃ appears to be that of Dharmatti *et al.* in 1965.¹⁵ Although experimental details are sketchy, it appears that the ⁵⁹Co NMR measurements were carried out on a powder sample in applied magnetic fields of less than 1 T. The authors reported a nuclear quadrupolar coupling constant, χ , of 5.5 MHz. Nine years later, Reynhardt published the results of a ⁵⁹Co NMR study of a single crystal of Co(acac)₃.¹⁶ Data were acquired at three different applied magnetic fields in the range 0.85–1.6 T. Only the central, $1/2 \leftrightarrow -1/2$, ⁵⁹Co NMR transition was monitored as a function of crystal orientation in the applied magnetic field. The results of this study yielded $\chi = 9.26 \pm 0.01$ MHz, with an asymmetry $\eta = 0.90 \pm 0.01$, and a span of the chemical shift tensor, Ω , of 1230 ppm. The orientations of the EFG and CS tensors were found to be non-coincident. Reynhardt attributed the discrepancy in his value of χ and that of Dharmatti *et al.*¹⁵ as arising from the latter authors' failure to consider the chemical shift anisotropy. Eaton and co-workers¹⁷ obtained ⁵⁹Co NMR spectra for a static powder sample of Co(acac)₃ at 11.75 T. The spectrum that they reported appears to be axially symmetric with $\Omega \approx 250$ ppm. The authors indicated that the spectrum they calculated using the quadrupolar and shift tensor components reported by Reynhardt¹⁶ is broader by more than an order of magnitude than that observed! More recently, Hayashi has used static and variable-angle spinning (VAS) ⁵⁹Co NMR spectra to investigate the EFG and CS tensors of powder samples of Co(acac)₃.¹⁸ Measurements were carried out at 9.4 T, and analysis of the ⁵⁹Co NMR spectra yielded the following results: $\chi = 5.6 \pm 0.1$ MHz, $\eta = 0.20 \pm 0.03$, $\Omega = 1159$ ppm. The EFG and CS tensors were found to be essentially coincident within experimental error. The results were not discussed in

* Author to whom correspondence should be addressed: phone, 902-494-2564; fax, 902-494-1310; e-mail, Roderick.Wasylishen@Dal.Ca.

[†] Dalhousie University.

[‡] McMaster University.

[⊗] Abstract published in *Advance ACS Abstracts*, July 1, 1997.

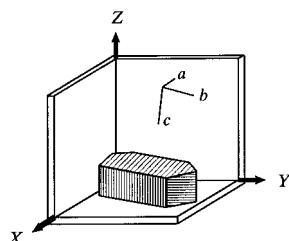


Figure 1. Illustration of the relative orientations of the monoclinic crystal axis system, *abc*, and the crystal holder, referred to as the orthogonal NMR cube frame *XYZ*. The crystal *a* and *b* axes are contained in the *XY* plane of the crystal holder.

light of previous measurements. It should be noted that although NMR experiments on powder samples are, in principle, capable of providing the *relative* orientation of the EFG and CS tensors, they provide no information on the orientation of the interaction tensors relative to the molecular framework.

Finally, a number of ^{59}Co NMR relaxation studies of $\text{Co}(\text{acac})_3$ in solution have been reported. While it is generally agreed that the quadrupolar relaxation mechanism is responsible for ^{59}Co spin–lattice and spin–spin relaxation in solution, the origin of the fluctuating EFG is not clear. In a 1979 publication, Doddrell *et al.* concluded that rotational motion of the $\text{Co}(\text{acac})_3$ molecule is not intimately involved in the ^{59}Co relaxation process; rather, excitations of the vibrational modes of the octahedron were considered to be the source of the fluctuations.¹⁹ Later, Grahn *et al.*²⁰ suggested that the efficiency of the ^{59}Co NMR relaxation is governed by modulations of the *static* quadrupolar tensor while Busse and Abbott²¹ explained that the relaxation rate for ^{59}Co in ostensibly symmetric complexes like $\text{Co}(\text{acac})_3$ can be accounted for by small *dynamic* distortions from ideal symmetry that fluctuate due to molecular reorientation. Most recent studies have assumed that the fluctuating EFG arises from rotational motion of the $\text{Co}(\text{acac})_3$ molecule.^{22,23} Using rotational correlation times derived from ^{13}C relaxation data and/or various “crude” hydrodynamic models, ^{59}Co nuclear quadrupole coupling constants ranging from 2.9 to 5.8 MHz have been derived. Clearly, it is of interest to establish the “static” ^{59}Co nuclear quadrupolar coupling tensor for solid $\text{Co}(\text{acac})_3$. In view of the large amount of ^{59}Co NMR data on $\text{Co}(\text{acac})_3$ and the discrepancies in the results, a re-examination of the single-crystal NMR data is in order.

Experimental Section

$\text{Co}(\text{acac})_3$ was obtained commercially and used without further purification. Large crystals were grown at room temperature from a solution in acetone. A single crystal of dimensions $2 \times 2 \times 4$ mm was selected and glued into an alumina crystal holder. The axes normal to the solid faces of this crystal holder were labeled *X, Y, Z* in a right-handed fashion. This axis system shall henceforth be referred to as the “cube frame” (Figure 1). After the NMR experiment, the crystal in its holder was transferred to an X-ray goniometer designed for this purpose. The orientation of the crystal axis system with respect to the cube frame was determined using a Siemens P4 four-circle X-ray diffractometer. A total of 264 reflections were centered and indexed to the expected cell, space group $P2_1/c$.²⁴ The Euler angles relating the orthogonalized crystal axis system a^*bc to the cube frame are $\alpha = 327.7^\circ$, $\beta = 170.9^\circ$, and $\gamma = 357.6^\circ$, following the *ZYX* order of rotations;²⁵ errors are estimated to be less than 1° . The crystal axes *a* and *b* are contained in the *XY* plane of the crystal holder.

Single-crystal ^{59}Co NMR spectra were obtained at 96.112 MHz on a Bruker AMX-400 NMR spectrometer ($B_0 = 9.4$ T).

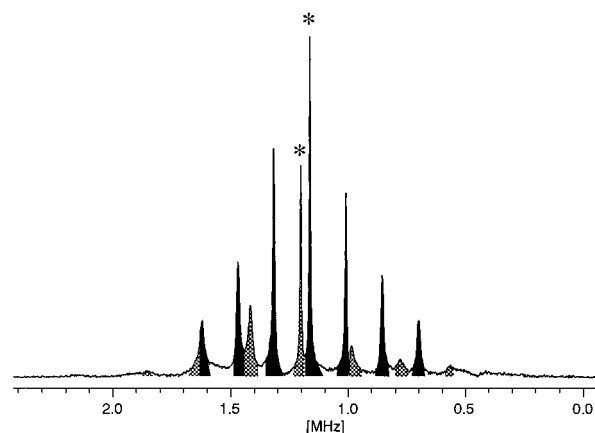


Figure 2. Single-crystal ^{59}Co NMR spectrum of $\text{Co}(\text{acac})_3$ obtained at 9.4 T. The central transitions of the two magnetically distinct sites A (black) and B (checked) are indicated by asterisks. This spectrum corresponds to the *Y* (126°) orientation in Figure 3.

Pulse widths were $1.2 \mu\text{s}$, with recycle delays of 2 s. A sweep width of 2.5 MHz and a time domain size of 12 K were employed. After Fourier transformation, spectra were processed in magnitude mode to overcome phase distortions. The single-crystal NMR spectra were obtained using an automated single-crystal NMR probe from Doty Scientific. For the *X* rotation, spectra were acquired in 9° intervals from 0 to 180° , while for *Y* and *Z* increments of 4.5° were used. For the *Y* and *Z* rotations, strong interference of the NMR response with the emission of a local FM radio station (96.5 MHz) was observed for orientations between 30° and 90° ; the weaker satellite peaks could not be observed in these areas. No interference was observed for other orientations.

All solid-state ^{59}Co NMR spectra were referenced with respect to an external concentrated aqueous solution of $\text{K}_3\text{Co}(\text{CN})_6$, with a frequency of 94.9407 MHz.

Results and Discussion

Crystal Structure and Single-Crystal ^{59}Co NMR Spectra.

The unit cell of the crystal structure of $\text{Co}(\text{acac})_3$ contains four crystallographically equivalent formula units. Crystallographic sites 1 and 2 are related by a center of inversion and constitute a pair of magnetically equivalent molecules. The same symmetry relation exists between sites 3 and 4. Each molecule from one pair of magnetically equivalent molecules is related to a molecule of the other pair *via* a 2-fold rotation or reflection. Molecules related by a 2-fold rotation or by reflection are magnetically nonequivalent.²⁶ Seven transitions are generally observed for each of the two magnetically distinct cobalt sites. A typical ^{59}Co NMR spectrum of the single crystal of $\text{Co}(\text{acac})_3$ is shown in Figure 2. The outer transitions ($7/2 \leftrightarrow 5/2$) and ($-5/2 \leftrightarrow -7/2$), were often separated by more than 1 MHz (see Figure 3). Because the B_1 field, ≈ 160 kHz, is much less than 1 MHz, the rf-pulses are by no means hard, nonselective pulses; hence the relative intensities of the various transitions are not proportional to $[I(I+1) - m(m+1)]$. For $I = 7/2$, the relative intensities would be 7:12:15:16:15:12:7 in this case. On the other hand, a selective pulse would yield transitions with relative intensities of $7^{1/2}:12^{1/2}:15^{1/2}:16^{1/2}:15^{1/2}:12^{1/2}:7^{1/2}$.²⁷ For the latter condition to hold, one would have to excite each individual transition without perturbing the others. In practice, the relative intensities of the various transitions will not follow either of these simple idealized distributions because the rf-pulse power is not uniform across the spectral width that one wishes to excite. Detailed theoretical treatments of how a spin $7/2$ system responds to rf pulses in the solid state are given elsewhere.²⁸ In addition

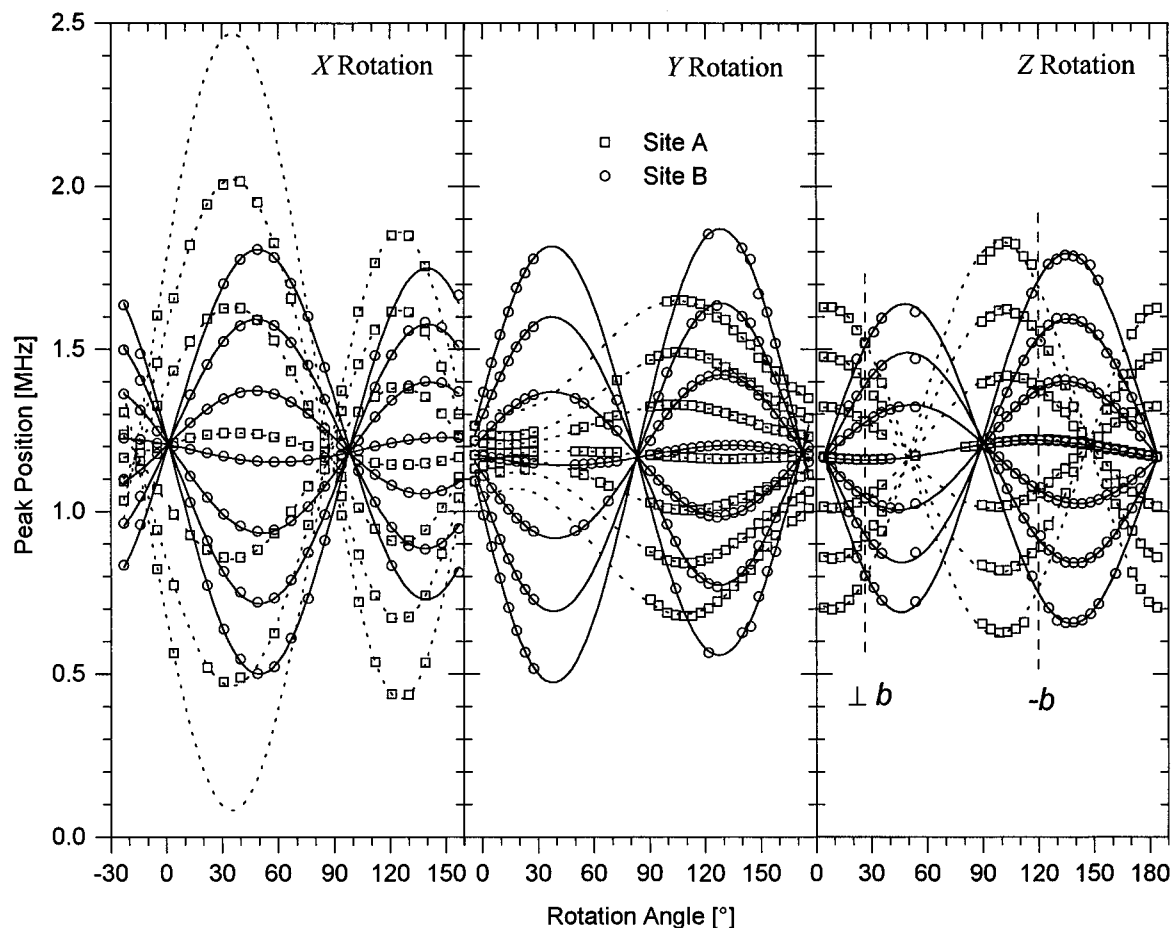


Figure 3. Observed peak positions, in MHz, relative to aqueous K₃Co(CN)₆, in the ⁵⁹Co NMR spectra of a single crystal of Co(acac)₃ as a function of the orientation of the cube holder in the external magnetic field. Rotations were performed about the cube X, Y, and Z axes, beginning with Y, Z, and X parallel to the external field, respectively. Two characteristic points can be identified from the Z rotation, at ca. 30° and 120°, where the crystal *b* axis is perpendicular and parallel, respectively, to the external magnetic field and both magnetically distinct sites become equivalent.

to the artifacts which arise from using neither nonselective nor selective pulses, it is important to recognize that the individual transitions may have different line widths.³ This might arise because of imperfections in the crystal. Qualitatively, the larger the frequency span of a particular transition, the larger its line width if the crystal is not perfect. The different transitions may also have different relaxation times in the solid state which, in principle, could lead to different line widths. Fortunately, the relative intensities of the seven single-quantum ⁵⁹Co NMR transitions of Co(acac)₃ are of little relevance to the present study since the focus of this investigation is to characterize the cobalt-59 EFG and CS tensors. Only the frequencies of observed transitions are important in characterizing these tensors. The observed peak positions for the single crystal of Co(acac)₃ as a function of the orientation of the crystal in the magnetic field are displayed in Figure 3. Before discussing the analysis of the more than one hundred spectra that we acquired, it is necessary to summarize the nuclear spin interactions which are important for cobalt-59 in Co(acac)₃.

Background Theory. The total Hamiltonian governing the ⁵⁹Co single-quantum NMR spectrum is composed of the Zeeman interaction, the chemical shift, and the nuclear quadrupolar interactions. The frequency of a given transition, *m* ↔ *m* - 1, can therefore be described as

$$\nu = \nu_0 + \nu^\sigma + \nu^{(1)}_{m,m-1} + \nu^{(2)}_{m,m-1} \quad (1)$$

where the Zeeman and isotropic chemical shift interactions are included in ν_0

$$\nu_0 = \frac{\gamma B_0}{2\pi} (1 - \sigma_{iso}) \quad (2)$$

and the anisotropic chemical shift interaction is given by

$$\nu^\sigma = \nu_0 (\delta_{11} \sin^2 \theta \cos^2 \phi + \delta_{22} \sin^2 \theta \sin^2 \phi + \delta_{33} \cos^2 \theta) \quad (3)$$

with the principal components of the CS tensor relative to the isotropic chemical shift, $\delta_{11} \geq \delta_{22} \geq \delta_{33}$, and the polar angles ϕ, θ describing the orientation of the external magnetic field in the principal axis system (PAS) of the CS tensor.

The nuclear quadrupole coupling is an electrostatic interaction between the nuclear quadrupole moment, eQ , and the EFG tensor, $e\mathbf{q}$, at the nucleus. In its PAS, the principal components of \mathbf{q} are defined in a right-handed fashion such that $|q_{33}| \geq |q_{22}| \geq |q_{11}|$. Because the quadrupolar interaction is traceless and symmetric, two parameters are sufficient to define the magnitude of the principal components, the quadrupolar coupling constant, χ , and the asymmetry parameter η :

$$\chi = e^2 Q q_{33} / h \quad (4)$$

$$\eta = \frac{q_{11} - q_{22}}{q_{33}} \quad (5)$$

In the case of Co(acac)₃, both first- and second-order quadrupolar terms will be considered:^{27,29-31}

$$\nu_{m,m-1}^{(1)} = \frac{\nu_Q}{4}(1 - 2m)[3 \cos^2 \vartheta - 1 + \eta \cos 2\varphi \sin^2 \vartheta] \quad (6)$$

$$\nu_{m,m-1}^{(2)} = \frac{\nu_Q^2}{12\nu_0} \left\{ \frac{3}{2} \sin^2 \vartheta [(A + B) \cos^2 \vartheta - B] - \eta \cos 2\varphi \sin^2 \vartheta [(A + B) \cos^2 \vartheta + B] + \frac{\eta^2}{6} [A - (A + 4B) \cos^2 \vartheta - (A + B) \cos^2 2\varphi (\cos^2 \vartheta - 1)^2] \right\} \quad (7)$$

with

$$\nu_Q = \frac{3\chi}{2I(2I - 1)} \quad (8)$$

$$A = 24m(m - 1) - 4I(I + 1) + 9 \quad (9)$$

$$B = \frac{1}{4}[6m(m - 1) - 2I(I + 1) + 3] \quad (10)$$

where the polar angles φ, ϑ describe the orientation of the external magnetic field in the PAS of the EFG tensor.

The frequencies of the six satellite peaks for each magnetic site are determined by the chemical shift and first- and second-order quadrupolar interactions, while the frequency of the central transition depends only on chemical shift and second-order quadrupolar interactions. Splittings between symmetric satellite peaks, $\Delta\nu_m = \nu_{m,m-1} - \nu_{1-m,-m}$, are affected only by the first-order quadrupolar interaction and can be used to derive the quadrupolar parameters (*vide infra*).

Analysis of Single-Crystal Data. The components of the quadrupolar tensor in the Zeeman frame were determined from the splitting between symmetric satellite peaks according to

$$e^2 Qq_{zz}(\psi)_i / h = \frac{7}{3} \Delta\nu_{7/2} = \frac{7}{2} \Delta\nu_{5/2} = 7 \Delta\nu_{3/2} \quad (11)$$

The quadrupolar splittings observed as a function of the crystal orientation, ψ , about an axis $i = X, Y, Z$ of the cube frame were then fit to the following equation (Figure 4):

$$e^2 Qq_{zz}(\psi)_i / h = A_i + B_i \cos 2\psi + C_i \sin 2\psi \quad (12)$$

The coefficients obtained from the three rotation patterns are collected in Table 1.

The quadrupolar tensor in the cube frame was then constructed from these coefficients as outlined by Volkoff *et al.*³² (eq 13). Diagonalization of the quadrupolar tensors constructed

$$\begin{aligned} e^2 Qq_{XX}/h &= (-2A_X + A_Y - B_Y + A_Z + B_Z)/3 \\ e^2 Qq_{YY}/h &= (-2A_Y + A_Z - B_Z + A_X + B_X)/3 \\ e^2 Qq_{ZZ}/h &= (-2A_Z + A_X - B_X + A_Y + B_Y)/3 \\ e^2 Qq_{XY}/h &= e^2 Qq_{YX}/h = -C_Z \\ e^2 Qq_{XZ}/h &= e^2 Qq_{ZX}/h = -C_Y \\ e^2 Qq_{YZ}/h &= e^2 Qq_{ZY}/h = -C_X \end{aligned} \quad (13)$$

in this manner gives the magnitudes of the quadrupolar interaction in its PAS and the direction cosines that describe the orientation of the PAS with respect to the cube frame. In order to obtain the principal components of the chemical shift tensor, the contribution of the second-order quadrupolar interac-

TABLE 1: Coefficients (in MHz) for the Linear Least-Squares Fit of the Cobalt-59 Quadrupolar Splittings for Sites A and B of Co(acac)₃ to Eq 12, with Standard Deviations in Units of the Least Significant Digits Given in Parentheses

parameter	site A	site B
A_X	1.060(7)	-0.325(12)
B_X	1.442(9)	0.420(18)
C_X	4.146(9)	-2.715(16)
A_Y	-1.319(10)	-0.063(12)
B_Y	0.749(14)	-0.749(15)
C_Y	0.574(15)	-3.011(16)
A_Z	0.340(13)	0.181(12)
B_Z	-2.386(16)	0.203(18)
C_Z	-0.770(21)	-2.429(17)

TABLE 2: Coefficients (in kHz) for the Linear Least-Squares Fit of the Cobalt-59 Chemical Shift Interaction of Sites A and B of Co(acac)₃ to Eq 14, with Standard Deviations in Units of the Least Significant Digits Given in Parentheses

parameter	site A	site B
A_X	1193.7(1)	1192.2(1)
B_X	14.1(2)	17.6(2)
C_X	48.0(2)	-34.8(2)
A_Y	1175.4(1)	1175.2(1)
B_Y	2.2(2)	-0.5(2)
C_Y	12.5(2)	-32.1(2)
A_Z	1191.9(2)	1190.7(2)
B_Z	-18.2(3)	-20.1(3)
C_Z	-27.4(3)	-24.9(3)

tion to the position of the central transition was computed, using the knowledge of the quadrupolar interaction in the cube frame. This orientation-dependent second-order shift was subtracted from the observed peak positions of the central transitions^{33,34} and the resulting pure chemical shift data were analyzed according to standard procedure.^{35,36} The positions were fit to an equation analogous to eq 12 (cf. Figure 5)

$$\nu(\psi)_i = A_i + B_i \cos 2\psi + C_i \sin 2\psi \quad (14)$$

and the chemical shift tensor in the cube frame was constructed from the coefficients summarized in Table 2 according to eq 15.³⁶

$$\begin{aligned} \delta_{XX} &= (A_Y - B_Y + A_Z + B_Z)/2 \\ \delta_{YY} &= (A_Z - B_Z + A_X + B_X)/2 \\ \delta_{ZZ} &= (A_X - B_X + A_Y + B_Y)/2 \\ \delta_{XY} &= \delta_{YX} = -C_Z \\ \delta_{XZ} &= \delta_{ZX} = -C_Y \\ \delta_{YZ} &= \delta_{ZY} = -C_X \end{aligned} \quad (15)$$

The next step of the analysis involves transforming the quadrupolar and chemical shift tensors from the cube frame to the crystal frame. This can be achieved using the orientation of the crystal axis system determined by X-ray diffraction. An internal check on consistency can be done by recognizing that the magnetically distinct tensors are related to each other *via* a C_2 operation. The orientation of this C_2 axis in the cube frame was calculated from the direction cosines of the EFG and CS tensors to be 0.4517 (210), 0.8420 (84), and 0.0166 (272), which agrees quite well (within 2°) with the orientation of the b axis obtained from the X-ray diffraction experiment: 0.4931, 0.8699, and -0.0844 (cf. Figure 3).

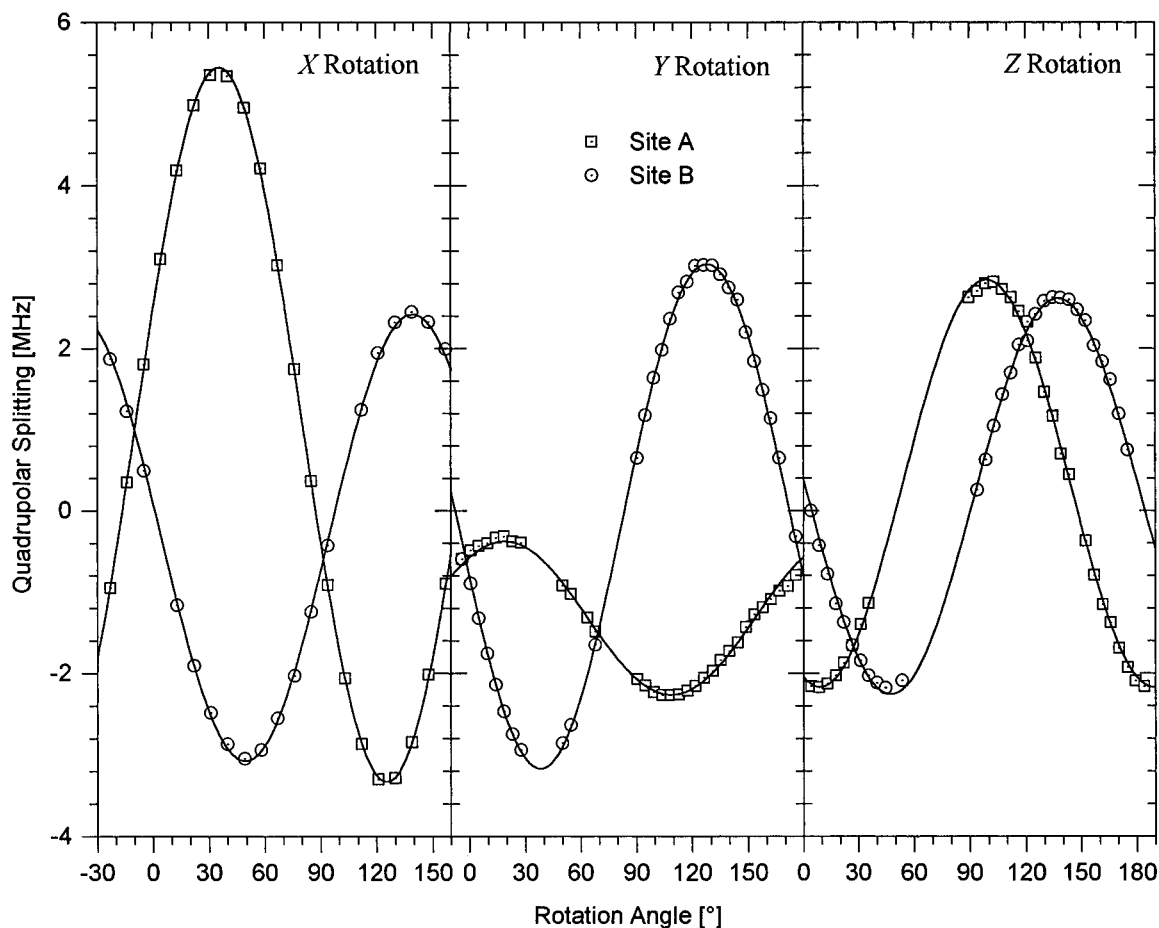


Figure 4. Cobalt-59 single-crystal NMR data at 9.4 T and least-squares curves for the quadrupolar splitting of Co(acac)₃ for rotations about the cube X, Y, and Z axes.

TABLE 3: Principal Components (in MHz)^a and Direction Cosines of the Averaged ⁵⁹Co Quadrupolar Tensor of Co(acac)₃ in the Crystal Axis Frame *a*bc*^b

components (MHz)	<i>a*</i>	<i>b</i>	<i>c</i>
e^2Qq_{11}/h	-2.159(37)	0.928(16)	0.351(6)
e^2Qq_{22}/h	-3.368(33)	-0.080(59)	0.517(24)
e^2Qq_{33}/h	5.527(70)	0.364(29)	-0.781(10)

^a This results in $\chi = 5.53$ MHz, $\eta = 0.219$. ^b The direction cosines are reported such that magnetic site B is assigned to crystallographic site 1. Direction cosines for site A can be generated by applying the symmetry operation (\bar{x}, y, \bar{z}) . Standard deviations in units of the least significant digits are given in parentheses.

Finally, the tensors associated with sites A and B must be assigned to the crystallographically equivalent sites 1,2 or 3,4. On the basis of the local symmetry at each cobalt nucleus, an approximate C_3 axis, one would anticipate that the unique component of the CS tensor, δ_{11} , would lie close to the C_3 axis.¹⁶ Recent high-level density functional calculations of the shielding tensor for Co(acac)₃ support this approximation.³⁷ Therefore, we assign the magnetic site B to crystallographic sites 1,2. For this assignment, the angle between the approximate C_3 axis and the unique component of the CS tensor is 4°; similarly, the angle with the largest component of the EFG tensor is 11° (for the alternate assignment, the angles are 63° for δ_{11} and 111° for e^2Qq_{33}/h). The final results for the averaged tensors in the orthogonalized crystal frame are summarized in Tables 3 and 4. The orientation of the tensors in the molecular frame of reference is illustrated in Figure 6. Errors in the orientation are estimated to be less than 5°.

TABLE 4: Principal Components (in ppm)^a of the Averaged ⁵⁹Co Chemical Shift Tensors of Co(acac)₃ in the Crystal Axis Frame *a*bc*^b

components (ppm)	<i>a*</i>	<i>b</i>	<i>c</i>
δ_{11}	698(22)	-0.140(42)	0.846(6)
δ_{22}	-222(12)	0.915(25)	0.310(56)
δ_{33}	-476(5)	0.380(43)	-0.434(28)

^a Relative to the isotropic chemical shift, $\delta_{iso} = 12498(5)$ ppm. The isotropic shift is measured with respect to aqueous $K_3Co(CN)_6$. ^b The direction cosines are reported such that the magnetic site B is assigned to the crystallographic site 1. Direction cosines for site A can be generated by applying the symmetry operation (\bar{x}, y, \bar{z}) . The Euler angles required to transform from the quadrupolar tensor to the chemical shift tensor are $\alpha = 72.4^\circ$, $\beta = 86.4^\circ$, and $\gamma = 12.9^\circ$. Standard deviations in units of the least significant digits are given in parentheses.

Quadrupolar Interaction. The magnitudes of the principal components for the ⁵⁹Co nuclear quadrupolar coupling tensor obtained here ($\chi = 5.53$ MHz, $\eta = 0.219$) are in excellent agreement with the values recently reported by Hayashi¹⁸ ($\chi = 5.6$ MHz, $\eta = 0.20$), but in poor agreement with the results of Reynhardt¹⁶ ($\chi = 9.26$ MHz, $\eta = 0.90$). Also, our result for χ is in good agreement with the value first reported by Dharmatti *et al.*¹⁵ ($\chi = 5.5$ MHz). Given that the latter value was estimated from the asymmetric line width of a powder pattern observed in an applied field where the ⁵⁹Co Larmor frequency was 10 MHz or less, the agreement is probably fortuitous. We have made some effort to understand the reason for the lack of agreement between our results and those of Reynhardt.¹⁶ Using our experimental results, we can qualitatively reproduce the rotation plots shown in Figure 2 of his paper; however, using

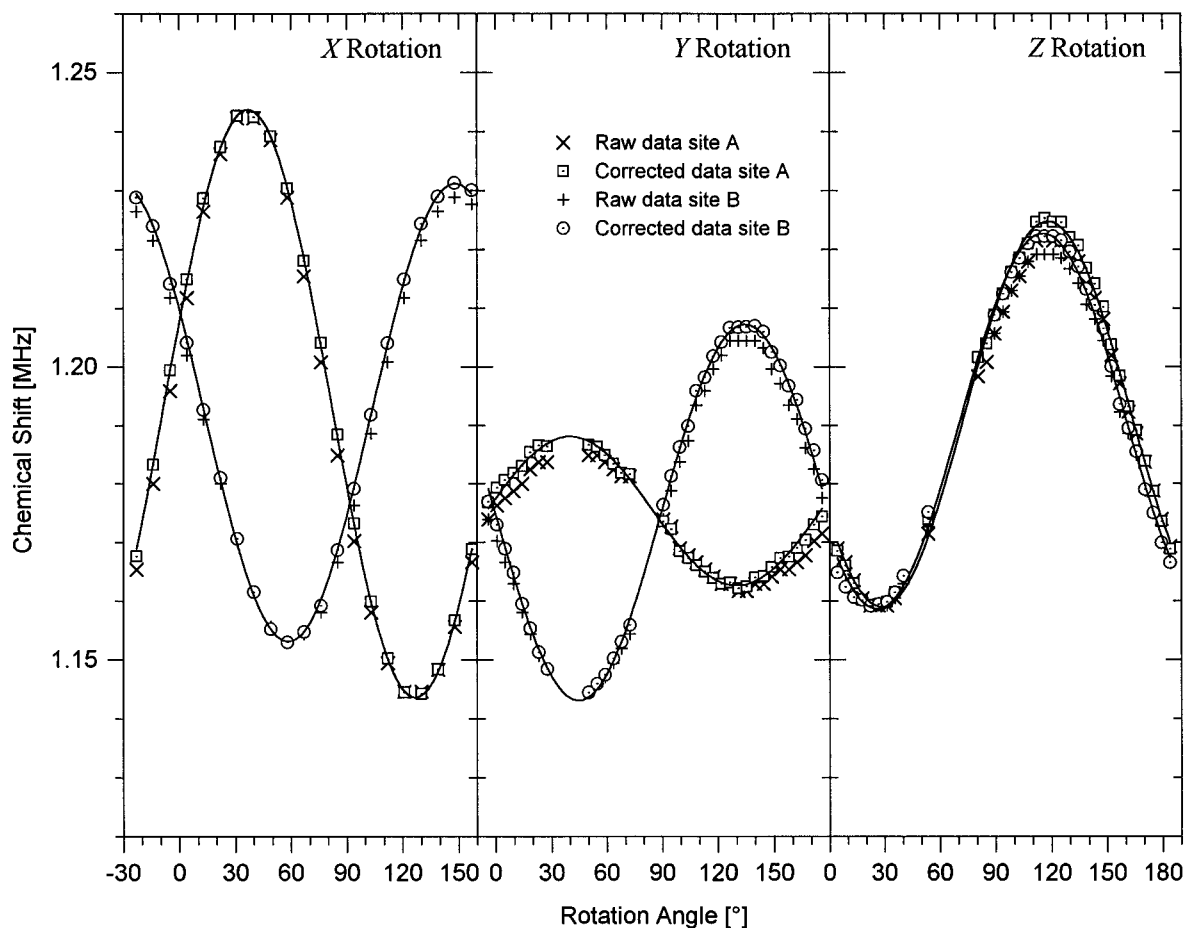


Figure 5. Cobalt-59 single crystal NMR data at 9.4 T and least-squares curves for the position of the central transition of $\text{Co}(\text{acac})_3$, in MHz, relative to aqueous $\text{K}_3\text{Co}(\text{CN})_6$, for rotations about the cube X, Y, and Z axes. The crosses and pluses correspond to observed positions, while the squares and circles represent the positions corrected for the second-order quadrupolar shift.

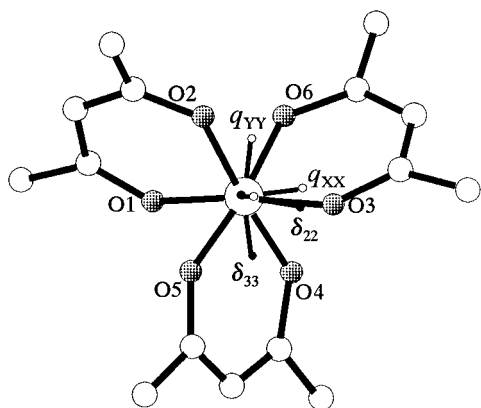


Figure 6. Orientation of the EFG and CS tensors in the molecular frame of $\text{Co}(\text{acac})_3$. The view is down the local C_3 axis. The direction of least shielding, δ_{11} , and the largest component of the electric field gradient tensor are approximately perpendicular to the paper plane. Hydrogen atoms have been omitted for clarity.

the coefficients that are given in Table 2 of ref 16, the agreement between the calculated and observed rotation plots is not as good, particularly for the rotation about the crystal a^* axis. It appears that there is an error in his analysis of the quadrupolar parameters. Certainly, on the basis of the approximate C_3 symmetry at cobalt, the asymmetry parameter obtained here is much more satisfying than that reported by Reynhardt.

Given the fair agreement between the quadrupolar coupling constant from solution relaxation measurements and our solid-state value, it is reasonable to assume that the EFG at the cobalt nucleus arises mainly from the six directly bonded oxygens. In

any case, it is clear that any interpretation of ^{59}Co NMR relaxation must be based on a model that includes a static electric field gradient. Even at sites with symmetry O_h , quadrupolar relaxation through asymmetric vibrations is not efficient.³⁸

A final note concerning the quadrupolar coupling constant is necessary: its sign cannot be determined from our single-crystal NMR experiment and was, therefore, arbitrarily set positive. The sign of the quadrupolar coupling constant could, in principle, be determined from a magic angle spinning (MAS) spectrum of a spin- $1/2$ nucleus, *e.g.*, ^{13}C , coupled to the ^{59}Co *via* the effect of the residual ^{13}C , ^{59}Co dipolar coupling.³⁹ Calculations show, however, that the effect on the ^{13}C NMR line shape would be rather small and uncharacteristic (<9 Hz at 4.7 T), primarily because of the large internuclear separation and the unfavorable angular terms.

Cobalt-59 Chemical Shift. The principal components of the chemical shift tensor obtained here are in good agreement with those obtained from ^{59}Co NMR studies of powder samples.^{18,40} The values reported by Hayashi¹⁸ ($\delta_{\text{iso}} = 12505 \pm 1$ ppm, with principal components relative to δ_{iso} of $\delta_{11} = 686$ ppm, $\delta_{22} = -213$ ppm, $\delta_{33} = -473$ ppm) are within experimental error of the values given in Table 4. Interestingly, the principal components of the shift tensor deduced by Reynhardt¹⁶ (relative to δ_{iso} , $\delta_{11} = 720 \pm 10$ ppm, $\delta_{22} = -210 \pm 10$ ppm, $\delta_{33} = -510 \pm 10$ ppm) are also in fair agreement with our values—the largest discrepancy being in δ_{33} where the difference is 34 ppm.

As mentioned in the introduction, Eaton *et al.*¹⁷ were unable to rationalize the ^{59}Co NMR spectrum they obtained for $\text{Co}(\text{acac})_3$ at 11.75 T, with a span of 250 ppm, using the data reported by Reynhardt.¹⁶ At 11.75 T, second-order quadrupolar

effects are not expected to be large even if the quadrupolar coupling constant is as large as 10 MHz. Calculations of powder line shapes using the quadrupolar and shift tensor parameters obtained in our work indicate that Eaton *et al.*¹⁷ observed only the low-frequency portion of the powder pattern arising from the central transition (note that $\delta_{22} - \delta_{33} = 256$ ppm). At 11.75 T, the span of the chemical shift tensor is approximately 140 kHz. Clearly, the rf-pulse power of the high-resolution spectrometer used in this study was insufficient to excite the entire central transition.

As already indicated, the unique component of the shift tensor ($\delta_{11} = 698$ ppm relative to the isotropic shift) lies very close to the C_3 axis. The intermediate component ($\delta_{22} = -222$ ppm) lies in the O–Co–O plane containing the two shortest Co–O bonds. The significance of this observation is unclear at present.

The interpretation of cobalt NMR chemical shifts has attracted considerable attention in the literature. Early in the history of solution NMR it was recognized that variations in ⁵⁹Co NMR resonance frequencies were related to the wavelength of the lowest-frequency optical-absorption maximum, λ . The longer the wavelength of the absorption maximum, the greater the resonance frequency. Griffith and Orgel¹² and Freeman, Murray, and Richards¹³ provided an interpretation for these observations based on Ramsey's magnetic shielding theory⁴¹ and crystal-field theory. They proposed that the cobalt magnetic shielding is related to the crystal-field splittings, Δ , obtained from electronic spectra by

$$\sigma = A - B/\Delta \quad (16)$$

where A is the diamagnetic shielding, predicted to be insensitive to the nature of the ligands, while the second term, the paramagnetic term, is given by

$$\frac{B}{\Delta} = \frac{8e^2\hbar^2}{mc^2} \langle r^{-3} \rangle_{3d} \Delta E(^1A_{1g} \rightarrow ^1T_{1g})^{-1} \quad (17)$$

The good correlation between σ and λ was certainly one of the early and most convincing successes of Ramsey's chemical shielding theory.⁴¹ Over the years, many workers have refined the expression describing the paramagnetic term, eq 17. The prime motivation of much of this work has been to obtain improved straight-line plots of measured chemical shifts *vs* energies derived from electronic spectra. Extensive reviews of this literature can be found elsewhere.^{14,42} Here, we mention only that some efforts to consider the effects of metal–ligand covalency have been made.^{43,44} Furthermore, the importance of considering departures from perfect octahedral symmetry has been recognized.^{44–46} For Co(III) complexes with D_3 symmetry such as Co(acac)₃, Juranić has shown that two excited electronic states must be considered⁴⁷

$$\sigma^p(D_3) = \frac{-8\mu_0\mu_B^2}{\pi} \langle r^{-3} \rangle_{3d} \left[\frac{\eta(^1A_2)}{3\Delta E(^1A_2)} + \frac{2\eta(^1E)}{3\Delta E(^1E)} \right] \quad (18)$$

where μ_0 is the permeability of free space, μ_B the Bohr magneton, and $\langle r^{-3} \rangle_{3d}$ the d orbital radial parameter in a free d⁶ ion. Within the framework of this model, anisotropy in the shielding results from differences in $\Delta E(^1A_2)$ and $\Delta E(^1E)$ and in the covalency parameters $\eta(^1A_2)$ and $\eta(^1E)$. The energies $\Delta E(^1A_2)$ and $\Delta E(^1E)$ have been estimated to be 16 250 and 17 150 cm⁻¹, respectively.⁴⁸ Qualitatively, if one assumes the covalency parameters $\eta(^1A_2)$ and $\eta(^1E)$ to be the same, the unique component of the axially symmetric shielding tensor is predicted to be the least shielded component, because $\Delta E(^1A_2)$ is less than $\Delta E(^1E)$, in agreement with experiment. Also, from

the slope of a plot of ⁵⁹Co chemical shift *vs* λ in Co(III) complexes containing oxygen and nitrogen donor ligands, the anisotropy of the chemical shift tensor for Co(acac)₃ is estimated to be 1250 ppm. More rigorous interpretations of the cobalt shift tensor in Co(acac)₃ will have to await the results of modern quantum chemical calculations that are beginning to emerge.

Acknowledgment. We thank Mr. Scott Kroeker, Ms. Katherine N. Robertson, and Dr. Sergey Sereda for their assistance and for several helpful comments. Also, we thank Professor Steve C. F. Au-Yeung for his interest in this work. NSERC of Canada is gratefully acknowledged for their support of this research in the form of operating and equipment grants (R.E.W.). R.E.W. acknowledges the Canada Council for a Killam Research Fellowship.

References and Notes

- (1) *NMR and the Periodic Table*; Harris, R. K., Mann, B. E., Eds.; Academic Press: London, 1978.
- (2) Medek, A.; Sachleben, J. R.; Beverwyk, P.; Frydman, L. *J. Chem. Phys.* **1996**, *104*, 5374.
- (3) Vosegaard, T.; Skibsted, J.; Bildsøe, H.; Jakobsen, H. J. *J. Magn. Reson., Ser. A* **1996**, *122*, 111.
- (4) Skibsted, J.; Vosegaard, T.; Bildsøe, H.; Jakobsen, H. J. *J. Phys. Chem.* **1996**, *100*, 14872.
- (5) Kempgens, P.; Hirschinger, J.; Elbayed, K.; Raya, J.; Granger, P.; Rosé, J. *J. Phys. Chem.* **1996**, *100*, 2045.
- (6) Shore, J. S.; Wang, S. H.; Taylor, R. E.; Bell, A. T.; Pines, A. *J. Chem. Phys.* **1996**, *105*, 9412.
- (7) Kroeker, S.; Eichele, K.; Wasylshen, R. E.; Britten, J. F. *J. Phys. Chem.*, in press.
- (8) Jameson, C. J. In *Nuclear Magnetic Resonance—A Specialist Periodical Report*; Vol. 25; Webb, G. A., Ed.; Royal Society of Chemistry: Cambridge, Great Britain, 1996, and previous volumes in this series.
- (9) *Nuclear Magnetic Shieldings and Molecular Structure*; Tossell, J. A., Ed.; Kluwer Academic Publishers: Dordrecht, The Netherlands, 1993; NATO ASI Series C, Vol. 386.
- (10) Ditchfield, R. In *Critical Evaluation of Chemical and Physical Structural Information*; Lide, D. R., Paul, M. A., Eds.; National Academy of Sciences: Washington, DC, 1974; pp 565–590.
- (11) Proctor, W. G.; Yu, F. C. *Phys. Rev.* **1951**, *81*, 20.
- (12) Griffith, J. S.; Orgel, L. E. *Trans. Faraday Soc.* **1957**, *53*, 601.
- (13) Freeman, R.; Murray, G. R.; Richards, R. E. *Proc. R. Soc. London* **1957**, *A242*, 455.
- (14) (a) Kidd, R. G. *Annu. Rep. NMR Spectrosc.* **1980**, *10A*, 1. (b) Laszlo, P. In *NMR of Newly Accessible Nuclei*; Laszlo, P., Ed.; Academic Press: New York, 1983; Vol. 2, pp 253–274. (c) Kidd, R. G. In *The Multinuclear Approach to NMR Spectroscopy*; Lambert, J. B., Riddell, F. G., Eds.; Reidel Publishing Co.: Dordrecht, The Netherlands, 1983; NATO ASI Series C, Vol. 103, pp 445–456. (d) Pregosin, P. S. In *Transition Metal Nuclear Magnetic Resonance*; Pregosin, P. S., Ed.; Elsevier: Amsterdam, 1991; pp 144–176.
- (15) Dharmatti, S. S.; Saraswati, V.; Vijayaraghavan, R. In *Proc. XIIIth Colloque Ampère*; van Gerven, L., Ed.; North-Holland Publishers: Amsterdam, 1965; pp 133–140.
- (16) Reynhardt, E. C. *J. Phys. C: Solid State Phys.* **1974**, *7*, 4135.
- (17) Eaton, D. R.; Buist, R. J.; Sayer, B. G. *Can. J. Chem.* **1987**, *65*, 1332.
- (18) Hayashi, S. *Magn. Reson. Chem.* **1996**, *34*, 791.
- (19) Doddrell, D. M.; Bendall, M. R.; Healy, P. C.; Smith, G.; Kennard, C. H. L.; Raston, C. L.; White, A. H. *Aust. J. Chem.* **1979**, *32*, 1219.
- (20) Grahn, H.; Edlund, U.; Holak, T. A. *Magn. Reson. Chem.* **1987**, *25*, 497.
- (21) Busse, S. C.; Abbott, E. H. *Inorg. Chem.* **1989**, *28*, 488.
- (22) Kanakubo, M.; Ikeuchi, H.; Satō, G. P. *J. Magn. Reson., Ser. A* **1995**, *112*, 13; *J. Mol. Liq.* **1995**, *65/66*, 273.
- (23) Kirby, C. W.; Puranda, C. M.; Power, W. P. *J. Phys. Chem.* **1996**, *100*, 14618.
- (24) Kruger, G. J.; Reynhardt, E. C. *Acta Crystallogr.* **1974**, *B30*, 822.
- (25) Man, P. P. In *Encyclopedia of Nuclear Magnetic Resonance*; Grant, D. M., Harris, R. K., Eds.; John Wiley & Sons: Chichester, UK, 1996; Vol. 6, pp 3838–3848.
- (26) Haebleren, U. *High-Resolution NMR in Solids, Selective Averaging*; Advances in Magnetic Resonance, Suppl. 1; Waugh, J. S., Ed.; Academic Press: New York, 1976.
- (27) Freude, D.; Haase, J. In *NMR, Basic Principles and Progress*; Diehl, P., Fluck, E., Günther, H., Kosfeld, R., Seelig, J., Eds.; Springer-Verlag: Berlin, 1993; Vol. 29, pp 1–90.

- (28) (a) Man, P. P.; Tougne, P. *Mol. Phys.* **1994**, *83*, 997. (b) Ageev, S. Z.; Sanctuary, B. C. *Mol. Phys.* **1995**, *84*, 835. (c) Ageev, S. Z.; Man, P. P.; Sanctuary, B. C. *Mol. Phys.* **1996**, *88*, 1277.
- (29) Stauss, G. H. *J. Chem. Phys.* **1964**, *40*, 1988.
- (30) Amoureux, J. P.; Fernandez, C.; Granger, P. In *Multinuclear Magnetic Resonance in Liquids and Solids—Chemical Applications*; Granger, P., Harris, R. K., Eds.; Kluwer Academic Publishers: Dordrecht, The Netherlands, 1990; pp 409–424.
- (31) Taulelle, F. In *Multinuclear Magnetic Resonance in Liquids and Solids—Chemical Applications*; Granger, P., Harris, R. K., Eds.; Kluwer Academic Publishers: Dordrecht, The Netherlands, 1990; pp 393–407.
- (32) Volkoff, G. M.; Petch, H. E.; Smellie, D. W. L. *Can. J. Phys.* **1952**, *30*, 270.
- (33) Scheubel, W.; Zimmermann, H.; Haerberlen, U. *J. Magn. Reson.* **1985**, *63*, 544.
- (34) Volkoff, G. M. *Can. J. Phys.* **1953**, *31*, 820.
- (35) Kennedy, M. A.; Ellis, P. D. *Concepts Magn. Reson.* **1989**, *1*, 35 and 109.
- (36) Power, W. P.; Mooibroek, S.; Wasylishen, R. E.; Cameron, T. S. *J. Phys. Chem.* **1994**, *98*, 1552.
- (37) Chan, J. C. C.; Au-Yeung, S. C. F. *J. Phys. Chem. A* **1997**, *101*, 3637. See also: Chan, J. C. C.; Au-Yeung, S. C. F.; Wilson, P. J.; Webb, G. A. *J. Mol. Struct. THEOCHEM* **1996**, *365*, 125.
- (38) Osten, H. J.; Jameson, C. J. *Mol. Phys.* **1986**, *57*, 553.
- (39) Harris, R. K.; Olivieri, A. C. *Prog. NMR Spectrosc.* **1992**, *24*, 435.
- (40) Chan, J. C. C., Ph.D. Thesis, Chinese University of Hong Kong, 1996.
- (41) Ramsey, N. F. *Phys. Rev.* **1950**, *78*, 699; **1952**, *86*, 243.
- (42) Juranić, N. *Coord. Chem. Rev.* **1989**, *96*, 253.
- (43) Juranić, N. *Inorg. Chem.* **1980**, *19*, 1093; *J. Chem. Phys.* **1981**, *74*, 3690.
- (44) Bramley, R.; Brorson, M.; Sargeson, A. M.; Schäffer, C. E. *J. Am. Chem. Soc.* **1985**, *107*, 2780.
- (45) Fujiwara, S.; Yajima, F.; Yamasaki, A. *J. Magn. Reson.* **1969**, *1*, 203.
- (46) Juranić, N.; Čelap, M. B.; Vučelić, D.; Malinar, M. J.; Radivojša, P. N. *J. Magn. Reson.* **1979**, *35*, 319.
- (47) Juranić, N. *J. Serb. Chem. Soc.* **1991**, *56*, 723.
- (48) Peacock, R. D. *J. Chem. Soc., Dalton Trans.* **1983**, 291.